Extending the Dispersive Optical Model to β-unstable Systems

Cole D. Pruitt[1,*], *Salvatore Simone* Perrotta[1], *Jutta* Escher[1], and *Oliver* Gorton[1]

[1]Lawrence Livermore National Laboratory, 7000 East Ave., Livermore, CA 94550, USA

Abstract. Phenomenological optical-model potentials (OMPs) are a key ingredient for nuclear cross section libraries that enter astrophysical nucleosynthesis simulations. While existing OMPs can reliably reproduce direct reaction cross sections on β-stable targets, the lack of scattering data on β-unstable targets limits the credibility of OMPs extrapolated to the extremely neutron-rich regime reached during explosive nucleosynthesis. Recent work with fully non-local dispersive OMPs indicates that even in regions where scattering data are unavailable, bound-state quantities, such as the proton and neutron number and binding energy, can serve as powerful constraints on the OMP. In this proceeding, we describe first steps toward a global, non-local, uncertainty-quantified, and fully dispersive OMP capable of leveraging both scattering and bound-state observables from stability to the driplines. As an example, we show how single-nucleon scattering data on traditional OMP training nuclei ^{40,48}Ca, ^{90}Zr, ^{112,124}Sn, ^{208}Pb can be combined with structural information to improve neutron capture cross sections at astrophysical energies relevant for the *i*-process and weak *r*-process.

1 Introduction

Optical-model potentials (OMPs) are essential for modeling many types of nuclear reaction, including the Hauser-Feshbach description of radiative capture. As a one-body description of a target nucleus as seen by an incident projectile, the OMP is a natural positive-energy analog to the shell model [1] and, if extended to negative energies, can be formally linked to the nucleon self-energy [2]. In direct reaction modeling, the OMP enters the Schrödinger equation directly, while in statistical Hauser-Feshbach calculations, the OMP enters as a transmission cofficient for formation of and particle decay from the compound state [3]:

$$\sigma_{\alpha\chi} = \sum_{J\pi} \sigma_{\alpha}^{CN}(E,J,\pi) G_{\chi}^{CN}(E,J,\pi) W_{\alpha\chi}(J), \qquad (1)$$

where $\sigma_{\alpha}^{CN}(E,J,\pi)$ is the probability for forming a compound state with spin J and parity π via entrance channel α, $G_{\chi}^{CN}(E,J,\pi)$ is the probability for exiting the compound state via exit channel χ, and $W_{\alpha\chi}(J)$ is a width fluctuation correction factor.

Near β-stability, the wealth of available single-nucleon scattering data tightly constrains the form of plausible OMPs and the transmission coefficients they generate. As such, modern phenomenological nucleon-nucleus OMPs agree closely where scattering data exist. However, the evolution of OMPs in isospin asymmetry as one moves away from β-stability is poorly constrained and remains an area of active interest. Contemporary efforts to better understand OMP asymmetry-dependence have employed charge-exchange data [4, 5], fission observables [6], isotopic ratios of neutron total cross sections [7], and charge radii/neutron skins [8–10]. Besides these phenomenological efforts, chart-wide microscopic and semi-microscopic OMPs have been developed [11, 12] based on density-folding approaches that do not require extrapolation from stability. Of these, the WLH OMP [11] is notable for providing uncertainties derived from truncation in the chiral effective interaction, an advance from past microscopic models with less rigorous uncertainty quantification. At present, however, microscopic models generally do not achieve phenomenological accuracy on known data [13], but they can serve as important guides on what forms phenomenological OMPs should assume when applied away from β-stability. Because direct neutron capture measurements on the most neutron-rich nuclides (e.g., ^{60}Ca, ^{78}Ni) are far beyond current experimental capabilities, our understanding of these reactions will be based solely on uncertainty-quantified theory for the foreseeable future.

Compared to traditional phenomenological OMP formulations, the dispersive optical-model (DOM) pioneered by Mahaux and Sartor [16, 17] offers several advantages. By enforcing an integral dispersion relation, a DOM potential eliminates certain arbitrary energy-dependence parameters in the functional form. Crucially, by extending to negative energies, the same potential can also describe bound-state properties of the target nucleus, such as single-particle energies. Several groups have developed DOM potentials along these lines [8, 18], and while most have focused on one or a few isotopes at a time, earlier this year a global DOM potential for neutron scattering was published [19]. In a series of analyses, the St. Louis DOM group has shown that, provided it is fully non-local, a DOM potential can generate the normalized one-body density from which many additional observables, including the overall nuclear binding energy, charge radius, and

*e-mail: pruitt9@llnl.gov

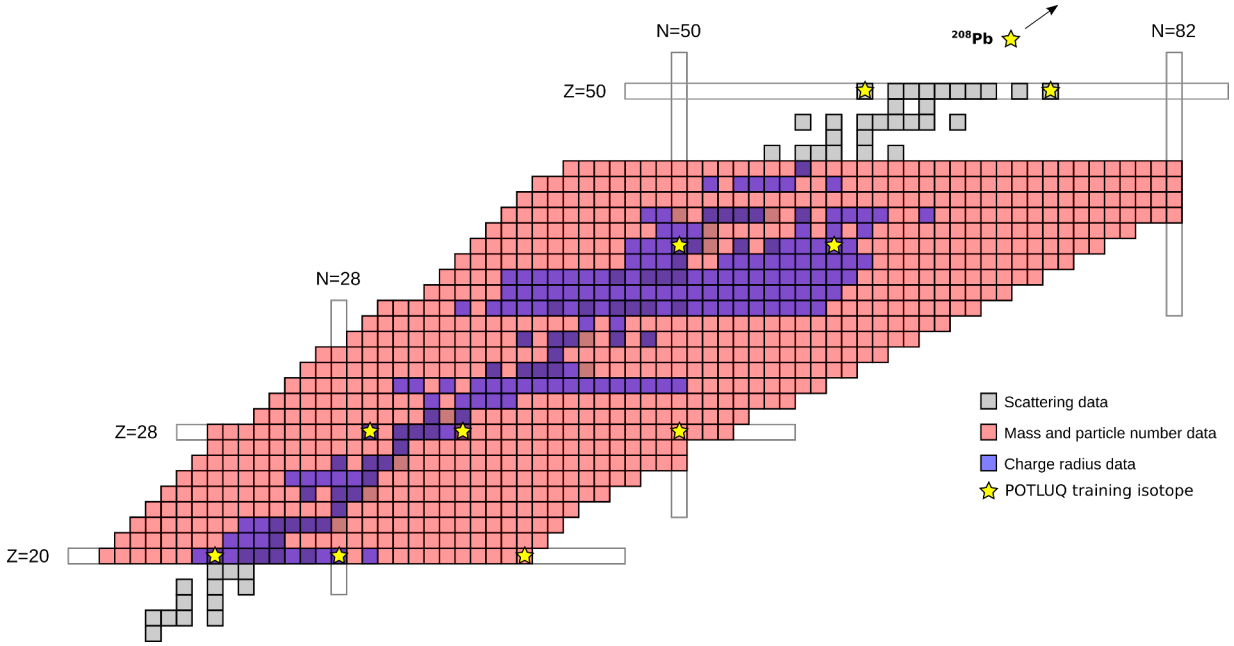

Figure 1. Scattering and bound-state data availability in the weak *r*-process region (Z=20-45). Gray squares represent isotopes for which at least some OMP-relevant single-nucleon scattering data are available in the EXFOR database [14]. Blue squares show charge radius data [15]. Red squares span the region where nuclear masses and/or particle numbers can be used as an OMP constraint. Stars show the "scaffold" isotopes used for training the POTLUQ potential.

proton and neutron number, can be extracted and compared with experiment [8, 10]. Dispersivity in the OMP is also needed to accurately describe rapid change of the real depth of the potential in the vicinity of the Fermi energy, an inevitable consequence of the strongly varying imaginary strength in this energy range. This physics matters for astrophysical and other low-energy ($E \lesssim 5$ MeV) applications, especially in near-dripline systems where the Fermi energy tends toward zero.

2 Next-generation OMPs

We argue that improving astrophysically relevant cross sections on highly asymmetric systems requires a new, fully non-local, chart-wide, dispersive phenomenological OMP. In the absence of scattering information on β-unstable systems, bound-state data (see Fig. 1) can constrain OMP parameters – but only if employed within a fully non-local, dispersive model. Because thousands of nuclei are expected to participate in the *r*-process, the reaction-theory ingredients for predicting cross section should be self-consistent and computationally inexpensive across a broad swath of the nuclear chart. Ideally, an OMP for this purpose should also be Lane-consistent so that the isovector potential can be readily computed and tested against relevant probes, such as quasielastic (p,n) scattering.

Besides possessing these physics features, a next-generation OMP should be equipped with robust uncertainty quantification. Because current level-density and gamma-ray-strength-function models also carry substantial uncertainties, quantifying the relative importance of OMP uncertainty on Hauser-Feshbach calculations can help disambiguate these sources from each other. Several recent efforts have explored uncertainty quantification in OMPs, including propagating these uncertainties into downstream applications (see [20]). Most recently, the Koning-Delaroche (KD) and Chapel-Hill '89 OMPs were equipped with well calibrated uncertainties [21] that were then applied to transfer and knock-out reactions in [22]. While radiative capture cross sections are typically computed with the Hauser-Feshbach formalism, in very neutron-rich environments (e.g., neutron star mergers), the underlying statistical assumptions may not apply, as only a handful of levels may be accessible. In this regime, direct reactions would dominate and accurate accounting of OMP uncertainty may become even more important.

In the following section, we introduce POTLUQ, an uncertainty-quantified non-local DOM under development at LLNL for chart-wide description of single-nucleon bound and scattering data. While we seek to eventually train against tens or hundreds of target nuclei simultaneously, here we perform initial parameter inference on a handful of "scaffold" nuclei, shown in Fig. 1. These systems are mostly singly- or doubly-magic, spherical, and with excellent experimental single-nucleon scattering coverage, making them especially useful for developing a global OMP functional form.

Model description. The POTLUQ potential is defined:

$$\begin{aligned}\mathcal{U}(E,r,r',l,j) = \mathcal{V}_v(r,r',l) - \mathcal{W}_v(E,r,r',l) \\ - \mathcal{W}_s(E,r,r',l) - \mathcal{V}_{so}(r,r',l,j) \\ + \mathcal{V}_c(r). \end{aligned} \quad (2)$$

In order, these are the real volume, imaginary volume, imaginary surface, and real spin-orbit terms, all non-local, plus the Coulomb term for protons. This form is similar to

those developed by the St. Louis group [8, 10] and Morillon et al. [19] but with slightly modified imaginary-surface and -volume energy dependences, allowing for greater asymmetry between particles and holes. We omit both the imaginary spin-orbit and real wine-bottle terms used in [7, 10]; though both terms are theoretically justified, neither appears to improve our description of the training data. The imaginary surface and volume terms consist of a Mahaux-Sartor-type energy-dependence times a radial Woods-Saxon (or its derivative) equipped with a Gaussian (Perey-Buck) nonlocality. All energy dependence in the real part comes from analytic dispersion integrals of the imaginary terms, making the potential fully dispersive. While the current formulation assumes spherical symmetry, future work will generalize to deformed systems via the coupled-channels formalism, following [18]. Based on parameter and volume-integral trends in [7, 10, 19], we were able to eliminate many parameters used in previous DOM forms that were not meaningfully constrained by training data. Once the global model is finalized, we intend to publish the complete parametrization details, including the relevant analytic dispersion integrals and their derivatives.

To perform parameter inference, we used the LLNL code COMMCAS [23], which employs EMCEE [24] under the hood for MCMC sampling. OMP and physics calculations were performed with TOMFOOL [21]. To coordinate parameter inference studies, S. S. Perrotta developed TOM.COM, an interface between the TOMFOOL and COMMCAS packages. Scattering cross sections were computed via a Lagrange-Legendre mesh calculable-*R*-matrix method with a first-order relativistic correction applied (see Appendix A of [21]). Bound-state observables were computed on a Lagrange-Laguerre mesh either by direct diagonalization of the Hamiltonian (for single-particle energies) or from sums over the one-body density matrix (for particle numbers, charge radii, and binding energies). Following [7, 9], we included a pairing correction for systems with partially occupied quasihole shells, enabling calculations on all even-even targets.

3 Results

For the preliminary model described here, our training data corpus consisted of:

- Binding energies [25], RMS charge radii [15], and nucleon numbers Z and N for ^{40,48}Ca, ^{90}Zr, ^{112,124}Sn, and ^{208}Pb
- Proton reaction cross sections (σ_{rxn}) from 10-65 MeV on ^{40}Ca, ^{90}Zr, and ^{208}Pb
- Neutron total cross sections (σ_{tot}) from 5-200 MeV on ^{40,48}Ca, ^{90}Zr, ^{112,124}Sn, and ^{208}Pb
- Neutron differential elastic cross sections from 10-55 MeV on ^{40}Ca, ^{90}Zr, and ^{208}Pb

The elastic, reaction, and total cross section data sets used were drawn from the KDUQ Corpus and Test Corpus of [21]. The preliminary version of POTLUQ introduced here achieves Koning-Delaroche-level agreement [26] for the scattering training data on all six training-data systems

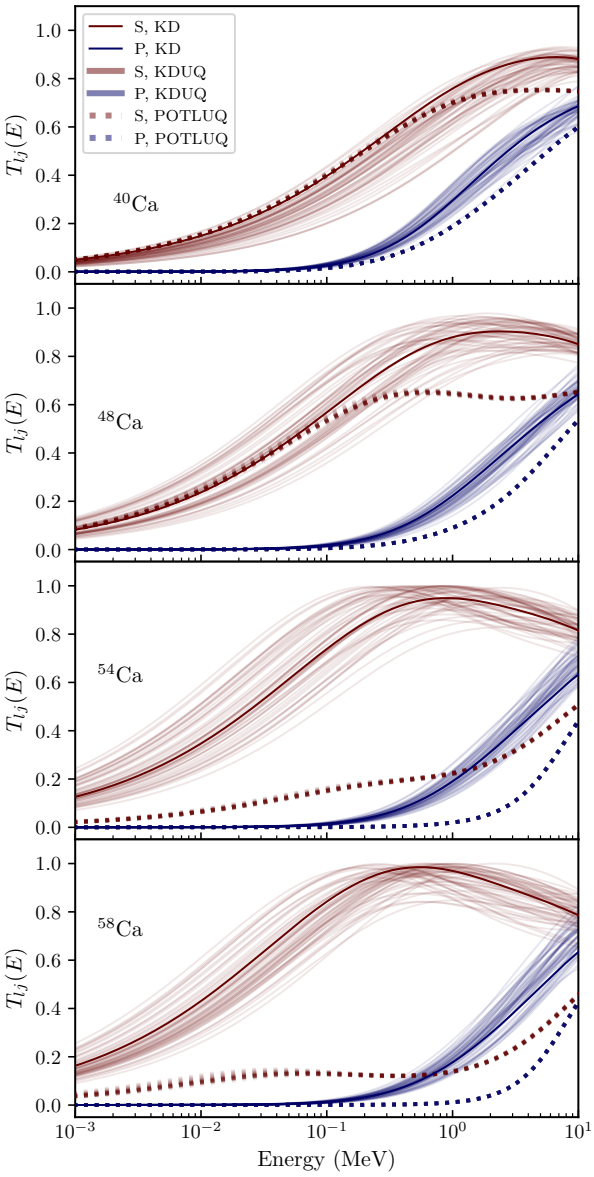

Figure 2. A comparison of *s*- and *p*-wave transmission coefficients computed with the KD [26], KDUQ[21], and POTLUQ OMPs for neutrons incident on Ca isotopes. To illustrate the uncertainty range spanned by the KDUQ and POTLUQ ensembles, fifty samples are plotted here for each OMP.

as well as an RMS-deviation of ≈2% across the bound-state observables listed above. Despite not fitting to proton elastic cross sections or proton and neutron analyzing powers, the model achieves near-Koning-Delaroche-level agreement for these quantities, indicating that the bound-state information (e.g., the charge radii) serves as a stringent constraint on the geometric parameters in the OMP.

To illustrate POTLUQ's utility for astrophysically relevant cross section predictions, we computed *s*- and *p*-wave transmission coefficients for neutron capture on ^{40,48,54,58}Ca, shown in Fig.2. While not shown here, we expect capture cross sections from full Hauser-Feshbach calculations to scale roughly linearly with these entrance-channel transmission coefficients, as illustrated

in [21]. Transmission coefficients computed using the KD OMP and its uncertainty-quantified extension, KDUQ, are shown for comparison. On the stable systems ^{40,48}Ca, POTLUQ is in overall agreement with KD/KDUQ, especially at incident energies below 1 MeV relevant for astrophysical temperatures at or below 10^9 K. As target neutron richness increases, traditional OMPs predict large, even increasing, *s*-wave transmission coefficients, corresponding to larger capture cross sections at high asymmetries. Given that the probability of neutron capture should tend toward zero as one reaches the dripline, the insensitivity to neutron richness indicates a physical problem when the KD and KDUQ models are extrapolated. In this case, the KD potential form includes a linear model for the Fermi energy that does not take asymmetry into account. While accurate enough near β-stability, it becomes increasingly unphysical in asymmetric systems. In contrast, POTLUQ predicts a severalfold reduction in transmission coefficient, in part due to its more realistic treatment of the Fermi energy as a function of asymmetry. Moreover, the uncertainty in POTLUQ is reduced compared to KDUQ; while we expect that POTLUQ's final uncertainties will likely end up larger than depicted here, the constraining power of bound-state training data on the geometric OMP parameters plays a key role in reducing uncertainties.

4 Conclusion

Credible, astrophysically relevant predictions for radiative capture on unstable systems requires a new generation of UQ-aware, fully non-local, Lane-consistent and dispersive OMPs. Such models could leverage both bound and scattering data where available and can be tested against a variety of isovector-sensitive probes, including charge exchange reactions, charge radii, neutron skin thicknesses, and fission observables. Building on recent DOM insights, we have developed a prototype model, POTLUQ, capable of accurately reproducing single-nucleon scattering and selected bound-state observables from A=40-208 and that shows dramatically different asymmetry-dependent behavior than traditional phenomenological OMPs. When finalized, we intend to propagate uncertainties from this next-generation OMP into neutron capture cross section libraries needed for weak *r*-process nucleosynthesis simulations to assess impact.

This work was performed under the auspices of the U.S. Department of Energy by Lawrence Livermore National Laboratory under Contract DE-AC52-07NA27344, with support from LDRD project 24-ERD-023.

References

[1] J.W. Holt, et al., in *Handbook of Nuclear Physics*, edited by I. Tanihata, H. Toki, T. Kajino (Springer, Singapore, 2020), pp. 1–30
[2] W. Dickhoff, R. Charity, Prog. Part. Nucl. Phys. **105**, 252 (2019). 10.1016/j.ppnp.2018.11.002
[3] J.E. Escher, et al., Rev. Mod. Phys. **84**, 353 (2012). 10.1103/RevModPhys.84.353
[4] A.J. Smith, et al., Phys. Rev. C **110**, 034602 (2024). 10.1103/PhysRevC.110.034602
[5] P. Danielewicz, et al., Nucl. Phys. A **958**, 147 (2017). 10.1016/j.nuclphysa.2016.11.008
[6] K. Beyer, Ph.D. thesis, University of Michigan (2024), https://dx.doi.org/10.7302/23750
[7] C.D. Pruitt, et al., Phys. Rev. C **102**, 034601 (2020). 10.1103/PhysRevC.102.034601
[8] M.H. Mahzoon, et al., Phys. Rev. Lett. **119**, 222503 (2017). 10.1103/PhysRevLett.119.222503
[9] C.D. Pruitt, et al., Phys. Rev. Lett. **125**, 102501 (2020). 10.1103/PhysRevLett.125.102501
[10] M.C. Atkinson, et al., Phys. Rev. C **101**, 044303 (2020). 10.1103/PhysRevC.101.044303
[11] T.R. Whitehead, et al., Phys. Rev. Lett. **127**, 182502 (2021). 10.1103/PhysRevLett.127.182502
[12] E. Bauge, et al., Phys. Rev. C **58**, 1118 (1998). 10.1103/PhysRevC.58.1118
[13] C. Hebborn, et al., J. Phys. G **50**, 060501 (2023). 10.1088/1361-6471/acc348
[14] Experimental Nuclear Reaction Data (EXFOR), online. Accessed 2022-07-06., https://www-nds.iaea.org/exfor/exfor.htm
[15] Nuclear Charge Radii, online. Accessed 2024-08-26., https://www-nds.iaea.org/radii/
[16] C. Mahaux, R. Sartor, in *Advances in Nuclear Physics* (Springer US, 1991), Vol. 20, pp. 1–223
[17] C. Mahaux, R. Sartor, Nucl. Phys. A **481**, 407 (1988). 10.1016/0375-9474(88)90336-3
[18] E.Sh. Soukhovitskiĭ, et al., Phys. Rev. C **94**, 064605 (2016). 10.1103/PhysRevC.94.064605
[19] B. Morillon, et al. (2024), arXiv:2403.05843, https://arxiv.org/abs/2403.05843
[20] A.E. Lovell, et al., J. Phys. G **48**, 014001 (2020). 10.1088/1361-6471/abba72
[21] C.D. Pruitt, J.E. Escher, R. Rahman, Phys. Rev. C **107**, 014602 (2023). 10.1103/PhysRevC.107.014602
[22] C. Hebborn, et al., Phys. Rev. Lett. **131**, 212503 (2023). 10.1103/PhysRevLett.131.212503
[23] O.C. Gorton, Ph.D. thesis, San Diego State University (2024), https://www.osti.gov/biblio/2301849
[24] D. Foreman-Mackey, et al., Publ. Astron. Soc. Pac. **125**, 306 (2013), 1202.3665. 10.1086/670067
[25] M. Wang, et al., Chin. Phys. C **45**, 030003 (2021). 10.1088/1674-1137/abddaf
[26] A.J. Koning, J.P. Delaroche, Nucl. Phys. A **713**, 231 (2003). 10.1016/S0375-9474(02)01321-0